Thermal Effect during Electromagnetic Pulse Welding Process

Thaneshan Sapanathan[1, a *], Kang Yang[1], Dmitrii Chernikov[2, b], Rija Nirina Raoelison[1, 3, c], Vladimir Gluschenkov[2], Nicolas Buiron[1, d] and Mohamed Rachik[1, e]

[1]Sorbonne universités, Université de technologie de Compiègne, Laboratoire Roberval, CNRS UMR 7337, Centre de Recherche Royallieu, CS 60319, 60203 Compiègne cedex, France

[2]Samara State Aerospace University, 34 Moskovskoye shosse, Samara, 443086, Russia

[3]Université de Bourgogne Franche Comté, IRTES-LERMPS, Université de Technologie de Belfort Montbéliard, 90100 Belfort, France

[a]thaneshan.sapanathan@utc.fr, [b]4ernikov82@mail.ru, [c]rija-nirina.raoelison@utbm.fr, [d]nicolas.buiron@utc.fr, [e]mohamed.rachik@utc.fr

* Corresponding author

Keywords: Electromagnetic welding; Numerical modeling; Temperature distribution; Plastic dissipation; Joule heating

Abstract. Magnetic pulse welding (MPW) is a solid state joining process, successfully utilized to join dissimilar metals. This advantage attracted manufacturing industries to fabricate hybrid materials to attain materials with a combination of multiple attributes. The high speed impact during the welding process causes various interfacial phenomena, which have been reported in previous research studies. Combined high speed collision, Joule heating due to eddy current and plastic heat dissipation cause noticeable heating in the workpiece. The heating from the plastic work and collision energy could particularly be significant at the vicinity of the interface compared to other regions of the workpiece. The Joule heating due to eddy current affects the entire workpiece that is prominent before the collision. There is a sharp increase of the temperature at the onset of weld formation due to dissipation of plastic work during the collision. 3D simulations of coupled electromagnetic-mechanical-thermal were carried out to investigate the heating due to the combined Joule heating and plastic dissipation. A case study of MPW, consist of a one turn coil combined with a field shaper, is used to investigate the welding process. The simulations were performed using LS-DYNA®, which has the capability of using both finite and boundary elements to solve the thermo-mechanical problem during electromagnetic forming. The predicted temperature distributions from numerical simulations show expected phenomena of Joule heating and plastic heat dissipation while the analytical approach used to estimate the localized increase in temperature due to supersonic gaseous compression. Minimizing the heating effect by identifying the influencing factors could help to optimize and control the quality of the magnetic pulse welded parts.

Introduction

Magnetic pulse welding process involves high speed collision and plastic deformation that enables to weld the metals at their solid state without creating a molten weld pool similar to that of during conventional welding processes. Therefore, MPW process enables to weld dissimilar metals, which are metallurgically incompatible for conventional techniques. The required collision speed is achieved by accelerating the work piece in an electromagnetic field, where significantly large Lorentz force excreted on the flyer part. The weldability criteria and suitable conditions for various materials can be found elsewhere [1-8].

Although, in general the MPW process is considered as a cold welding technique [1-3], resent research studies reveal possible heating and even potential melting at the interface of the MPWed joints [9-11]. Certainly, the localised increase in temperature has been evidenced under similar conditions during impact welding [12, 13], cold spray coating process [14] and solid particle erosion with impact response [15], where the favourable condition for the heating was reported. The onset criterion for the temperature increase and the occurrence of in situ melting has also been predicted experimentally and analytically using a viscous dissipation function in relation with impact conditions and material properties [12].

Moreover it is arguable, that the elevated local temperature could contribute towards the developments of interfacial phenomena such as oxide formation or burning of the jetting materials [10, 16-18] and formation of intermetallic compounds or intermediate phases at the interface [19, 20]. Formation of intermetallic compounds typically requires at least 50-80% of the melting temperature of the parent material [21]. Moreover, in recent studies finite element simulations with incorporated thermomechanical attribute are used to show temperature distributions along the interface and that has also been correlated to describe the local interfacial phenomena such as void formation and intermetallic region during impact welding processes [22, 23]. However, there was no empirical evidence of the temperature measurement to prove the increase in local temperature during the process. Although, those interfacial simulations qualitatively well predict the interfacial features including the potential failure mechanism of void formations under certain conditions that has been attributed with the localised increase in temperature during the process, the heating sources and the contribution of the each component are not been clearly investigated for MPW processes.

Multiple components of possible heating sources could be identified during a MPW process, including plastic deformation, Joule heating and collision energy dissipation during the impact. However, supersonic gaseous compression under high pressure is also suggested as another potential heating mechanism during a MPW process [3, 16]. The numerical simulation in this study was conducted without including the contribution of heating from supersonic gaseous compression. However, after the simulation, results with Joule heating and plastic dissipation was superimposed with the contribution of the supersonic compression based on an analytical approach suggested by Koschlig et al.[24]. This superpositioning approach allows the study to predict the total potential heating effect at the interface during the MPW process.

Materials and Method

The configuration of the MPW process and input current used in the coupled electromagnetic-mechanical-thermal simulation are shown respectively in Fig. 1a and 1b. Aluminum alloy AA2024-T351 is considered for both tube and rod in this study. Electromagnetic, mechanical and thermal properties of the materials used for the individual parts are given in Table 1. Simulations were carried out to investigate the heating effect using LS-DYNA® package with the solver version R8.

Both thermal and electromagnetic (EM) solvers work implicitly where at each electromagnetic time step the EM solver will communicate with an extra Joule heating term [25]. The calculated magnetic field and Lorentz forces are used in dynamic mechanical computing. A simplified Johnson-Cook constitutive model was used here to prescribe the material to capture the high strain rate behavior, written in Eq. 1.

$$\bar{\sigma} = (A + B\bar{\varepsilon}^n)\left[1 + C ln\left(\frac{\dot{\bar{\varepsilon}}}{\dot{\bar{\varepsilon}}_0}\right)\right] \quad (1)$$

This particular material model has a drawback of not including the softening effect and change in electrical conductivity while having an increase in temperature. However these simulations show a predictable global behavior of the temperature due to Joule effect and plastic heat dissipation while having a high strain rate deformation and onset of collision during the welding process. The heat transfer between parts and the surrounding environment was neglected because of the short duration of the processing time (i.e the process generally completes within the first half cycle of the current period). The initial temperature of the simulations was set to 298 *K*.

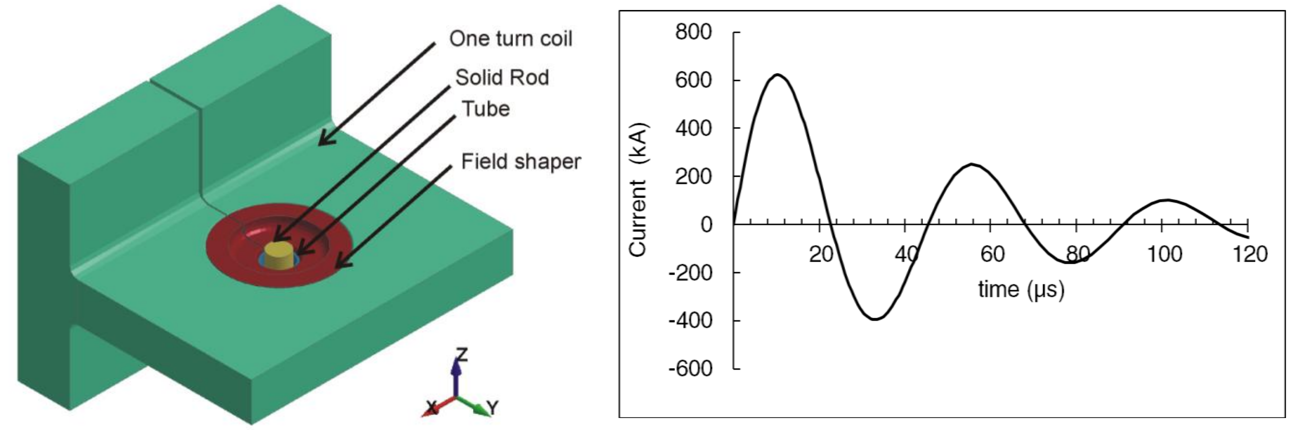

(a) (b)

Fig. 1. 3D model (a) and input current (b) used in the numerical simulations

Table 1: Mechanical, thermal and EM properties of materials used in this model for individual parts

Material	Part	Density (*kg/m*^{3})	Young's modulus (*GPa*)	Poison ratio	Electrical conductivity (*S/m*)	Specific heat capacity (*J/kg.K*)	Thermal conductivity (*W/m.K*)
AA2024 – T351	Tube and Rod	2700	73	0.33	1.74×10^7	795	143
Copper alloy	Fieldshaper	7900	210	0.29	2.66×10^7	486	36
Steel	Coil	Rigid			4.06×10^6	486	36

Table 2: Johnson-Cook parameters used for the aluminum alloy AA2024-T351

Johnson-Cook parameters	*A* (MPa)	*B* (MPa)	*C*	*n*
Numerical values	352	440	0.42	0.0083

Moreover the supersonic gaseous compression was estimated using the Eq.2 [24]. T_0 and T_1 are respectively the initial and final temperatures. The quantities α and β are respectively given in Eq. 3 and 4.

$$T_1 = T_0.\frac{(\alpha-\beta)(1+\beta(\alpha-\beta))}{\alpha} \quad (2)$$

$$\alpha = (1+\beta)M_0^2 \quad (3)$$

$$\beta = \frac{\gamma-1}{\gamma+1} \quad (4)$$

The M_0 and γ are respectively the Mach number of the shock wave and adiabatic index of gas (γ = 1.4 from kinematic theory for air at 0°C). The initial Mach number can be obtained by the ratio between the shock velocity and the speed of sound at the initial temperature, the shock speed (V_{shock}) for air can be calculated based on the expression of Hunoniot's relation with the collision speed (V_{col}) in meter per seconds using Eq. 5. Sound speed in the air is estimated at 25°C as 346.1 *m/s*.

$$V_{shock} = 899 + 0.939V_{col} \quad (5)$$

Results and discussion

The numerical simulations reveal the temperature distribution of the tube and rod are respectively shown in Fig. 2a and 2b. These results show the total heat due to Joule heating and plastic dissipation was obtained at a time step of 20.8μs (i.e at the end of first half cycle).

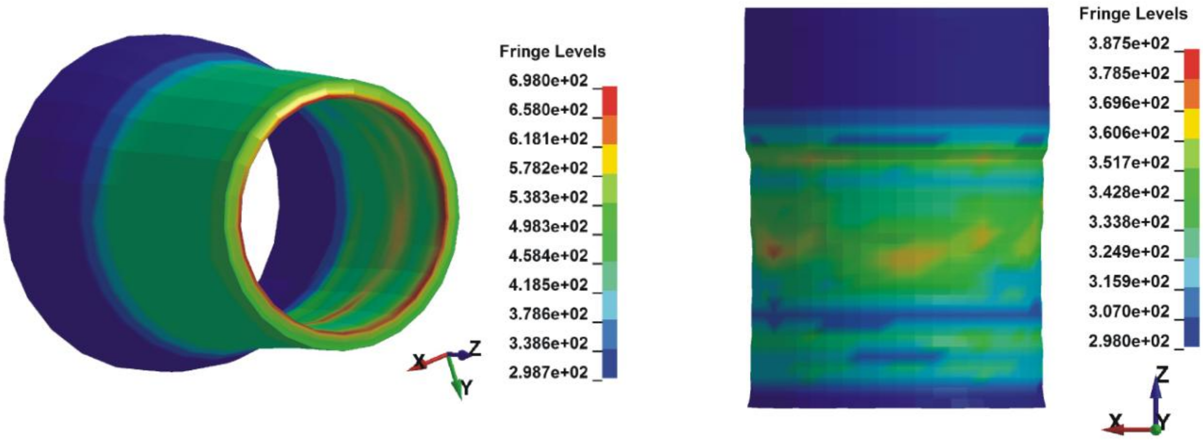

(a) (b)

Fig. 2. Global temperature distribution on the tube (a) and rod (b) at 20.8μs

Temperature against time for both tube and rod during first half period of the impulse current is also shown in Fig. 3a and 3b respectively. The region highlighted for the sudden increase in temperature during the collision. Although electric contact resistance at the onset of contact was considered as a heating source in various models, the heat contribution from this phenomenon was not significantly apparent during the simulations.

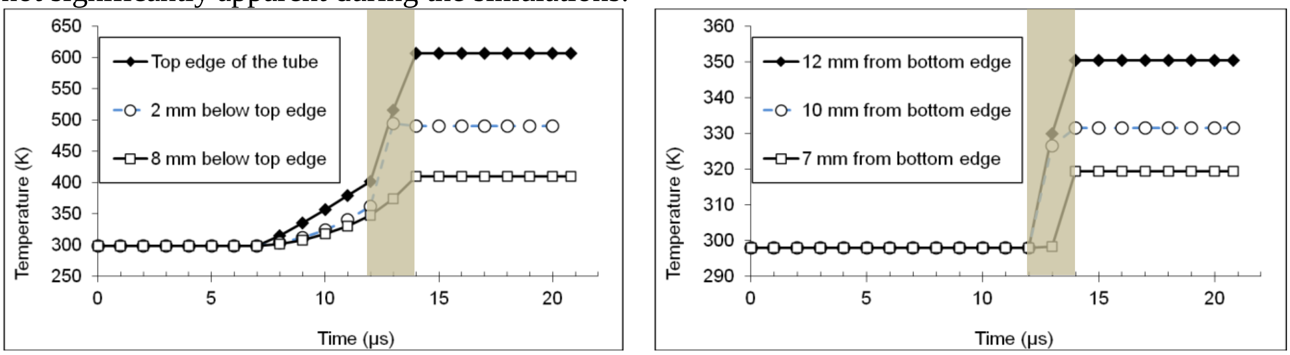

(a) (b)

Fig. 3. Temperature against time for the tube (a) and rod (b) obtained during the first half period of the impulse current at various locations, sharp increase in both tube and rod occurs during the onset of impact (i.e highlighted region), between ~12 – 14 μs.

The predictive equations (Eq. 2-5) indicate that there is a possibility of the final temperature to reach ~1211 *K* due to the supersonic gaseous compression alone. By superimposing this result with the global average temperature increase of ~222 *K* for the tube, the final temperature could reach ~1433 *K*. However, the shock front travels with an estimate speed of ~1390 *m/s*, which indicate the time duration affecting the metal due to the gaseous compression is very short, that may result the heating to be experienced only by ~100μm of the interface region. In order to simplify the interfacial investigation thermo-mechanical simulations without the electromagnetic effect were carried out in Abaqus package to further investigate the interfacial temperature using an estimate of the collision velocity of the process.

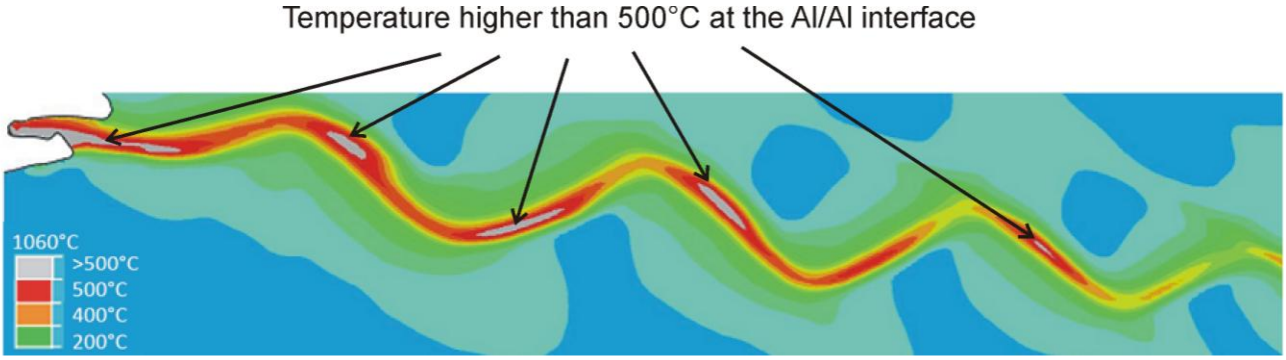

Fig. 4. Interfacial temperature distribution and wavy morphology obtained from numerical simulation at an Al/Al interface using thermo-mechanical approach using Abaqus Package.

The thermo-mechanical approach used in these simulations successfully predicts the interfacial temperature without the global Joule heating effect at the interface (Fig .4). This study clearly indicates the increase in interfacial temperature while the other regions do not show similar influence of thermal effect. Certain localized regions show a temperature of above 500°C (773 K) as an indication of possible melting during the MPW process (Fig .4).

Conclusions

3D Numerical simulations with electromagnetic-mechanical with thermal coupling were carried out to investigate the heating effect during a magnetic pulse welding process. The simulations well capture the global temperature distribution in the welding components, and they clearly represent the temperature increase due to Joule effect, heat dissipation during plastic deformation and heat increase due to collision energy. However, there may be a potential contribution of the interfacial heating due to high velocity impact and supersonic gaseous compression at the interface. Although the 3D models do not include the heating due to the supersonic gaseous compression, an analytical approach was used to estimate the heating effect due to the supersonic gaseous compression during the MPW process. Therefore, another simplified thermo-mechanical 2D model with thermal components were considered to investigate the interfacial heating effect during the process, which clearly capture the in situ heating at the interface, while this cannot include the global behavior of electromagnetic heating due to Joule effect. Therefore, when interpreting the heating mechanism of MPW, one should consider the different sources of heating and supper impose those multiple sources to estimate the interfacial heating effect. This study indicates the potential mechanisms of the heating during a MPW, while that could be used to optimize for a favorable welding condition of the metal components.

Acknowledgements

Authors would like to acknowledge the “Région Picardie” and “Le fonds européen de développement régional (FEDER)” for their financial support and “Plateforme Innovaltech” for their collaboration.

References

[1] V. Shribman, Magnetic Pulse welding for dissimilar and similar materials, 3rd Int. Conf. on High Speed Forming, Dortmund, 2008, 13-22.
[2] V. Shribman, Y. Livshitz, O. Gafri, Magnetic pulse welding and joining–a new tool for the automotive, SAE Tech. Pap., (2001) 01-3408.
[3] T. Aizawa, M. Kashani, K. Okagawa, Application of magnetic pulse welding for aluminum alloys and SPCC steel sheet joints, Weld. J., 86 (2007) 119-124.

[4] R. Raoelison, N. Buiron, M. Rachik, D. Haye, G. Franz, M. Habak, Study of the elaboration of a practical weldability window in magnetic pulse welding, J. Mater. Process. Technol., 213 (2013) 1348-1354.
[5] A. Kapil, A. Sharma, Magnetic pulse welding: an efficient and environmentally friendly multi-material joining technique, J. Cleaner Prod., 100 (2015) 35-58.
[6] R. Raoelison, N. Buiron, M. Rachik, D. Haye, G. Franz, Efficient welding conditions in magnetic pulse welding process, Journal of Manufacturing Processes, 14 (2012) 372-377.
[7] R. Raoelison, M. Rachik, N. Buiron, D. Haye, M. Morel, B. Dos Sanstos, *et al.*, Assessment of gap and charging voltage influence on mechanical behaviour of joints obtained by magnetic pulse welding, 5th Int. Conf. on High Speed Forming, Dortmund, 2012, 207-216.
[8] A. Lorenz, J. Lueg-Althoff, G. Göbel, C. Weddeling, E. Beyer, A. Tekkaya, Influence of Axial Workpiece Positioning during Magnetic Pulse Welding of Aluminum-Steel Joints, 6th Int. Conf. on High Speed Forming, South Korea, 2014.
[9] M. Marya, S. Marya, Interfacial microstructures and temperatures in aluminium–copper electromagnetic pulse welds, Sci. and Technol. Weld. Joining, 9 (2004) 541-547.
[10] A. Stern, O. Becher, M. Nahmany, D. Ashkenazi, V. Shribman, Jet Composition in Magnetic Pulse Welding: Al-Al and Al-Mg Couples MPW jet phenomena were investigated and jet material cornposition for similar Al alloys and two samples of dissimilar Al-Mg alloy couples were observed, Weld. J., 94 (2015) 257S-264S.
[11] R. N. Raoelison, T. Sapanathan, N. Buiron, M. Rachik, Magnetic pulse welding of Al/Al and Al/Cu metal pairs: Consequences of the dissimilar combination on the interfacial behavior during the welding process, Journal of Manufacturing Processes, 20, Part 1 (2015) 112-127.
[12] J. Robinson, Fluid mechanics of copper: viscous energy dissipation in impact welding, J. Appl. Phys., 48 (1977) 2202-2207.
[13] B. Crossland, Development of exlosive welding and its application in engineering, Metals materials, 5 (1971) 402-413.
[14] P. C. King, S. H. Zahiri, M. Jahedi, Focused ion beam micro-dissection of cold-sprayed particles, Acta Mater., 56 (2008) 5617-5626.
[15] D. R. Andrews, J. E. Field, Temperature dependence of the impact response of copper: erosion by melting, J. Phys. D: Appl. Phy., 15 (1982) 2357.
[16] P. Groche, C. Pabst, Numerical simulation of impact welding processes with LS-DYNA, 10th European LS-DYNA Conference, Würzburg, Germany, 2015.
[17] C. Pabst, P. Groche, Electromagnetic Pulse Welding: Process Insights by High Speed Imaging and Numerical Simulation, 6th Int. Conf. on High Speed Forming, South Korea, 2014, 77-88.
[18] S. Kakizaki, M. Watanabe, S. Kumai, Simulation and experimental analysis of metal jet emission and weld interface morphology in impact welding, Mater. Trans., 52 (2011) 1003-1008.
[19] M. Geyer, S. Böhm, Influence of contact surface on weldability with electromagnetic pulses, IIW Denver Annual Assembly, (2012)
[20] A. Stern, V. Shribman, A. Ben-Artzy, M. Aizenshtein, Interface Phenomena and Bonding Mechanism in Magnetic Pulse Welding, J. Mater. Eng. and Perform., 23 (2014) 3449-3458.
[21] N. F. Kazakov, Diffusion Bonding of material. Moscow: Mir Publishers, 1985.
[22] A. Nassiri, G. Chini, A. Vivek, G. Daehn, B. Kinsey, Arbitrary Lagrangian–Eulerian finite element simulation and experimental investigation of wavy interfacial morphology during high velocity impact welding, Mater. Des., 88 (2015) 345-358.
[23] W. Xu, X. Sun, Numerical investigation of electromagnetic pulse welded interfaces between dissimilar metals, Sci. and Technol. Weld. Joining, (2015) in press.
[24] M. Koschlig, D. Raabe, M. Veehmayer, Production of Steel-Light Metal Compounds with Explosive Metal Cladding, 3rd Int. Conf. on High Speed Forming, Dortmund, 2008.
[25] I. Çaldichoury, P. L'Eplattenier. (2012). EM Theory Manual.